Polymorphism of water in two dimensions

Tanglaw Roman and Axel Groß
Institute of Theoretical Chemistry, Ulm University, 89069 Ulm, Germany
(Dated: December 8, 2015)

The structure of confined water is governed by a delicate interplay between water-substrate and water-water interactions. Motivated by recent experimental studies on water in graphene nanocapillaries, two-dimensional water layers have been addressed by first-principles electronic structure calculations. In order to identify the structure-determining factors, first calculations for free-standing water layers have been performed. We demonstrate that two-dimensional water structures consisting of square bilayers, rhombic bilayers, truncated-square bilayers or secondary-prism bilayers are energetically more favorable than the traditionally considered hexagonal bilayer. These 2D water structures are stabilized by a compromise between high coordination and optimum tetrahedral bonding geometry. The identified structure determining factors responsible for the polymorphism of water in two dimensions will be operative in any confined water structure. The graphene-water interaction associated with the confinement of water within graphene sheets has an additional, but rather weak influence on the structural stability of water layers.

Water in a confined geometry at surfaces plays an enormously important role in many fields of natural sciences such a biology, (electro-)chemistry, materials science and earth science [1]. A basic understanding of the factors influencing the structure of the water layers is crucial for comprehending the function of water at interfaces, as interfacial water often exhibits properties that are distinctively different from those of bulk water [2–4]. The structure of the water layers directly at the solid-liquid interface is governed by an interplay between the water-water and the water-substrate interactions [5, 6]. Usually it is assumed that water at flat surfaces tends to form hexagonal ice-like layers [7], and only through the corrugation of the underlying substrate some other geometry might be imposed on the water layer [6, 8, 9].

Hence the recent high-resolution electron microscopy observation of *square* ice confined between two graphene sheets [10] was rather surprising as the water-graphene interaction exhibits only a weak dependence on the position and orientation of the water molecule [11, 12]. There is an ongoing discussion whether or not the transmission electron microscopy images [10] should be attributed to a film of square water or to accumulated salt sandwiched between graphene sheets [13, 14]. Still, this experimental study has raised interest in the fundamental question whether under ambient conditions two-dimensional water layers can realize geometries that are not feasible for bulk ice [15].

All experimentally observed two-dimensional water structures are subject to water-substrate interactions that influence their shape. On the other hand, theoretical studies allow to address two-dimensional water structures which are only subject to the water-water interactions. This allows to disentangle the influence of the water-water interaction from the water-substrate interaction [16–18]. Therefore we have performed a systematic study of the stability of free-standing water structures using first-principles electronic structure calculations based on density functional theory (DFT). In the DFT calculations we have employed the RPBE functional [19] together with dispersion corrections [20] which is known to give a reliable description of water properties [21] and the water-surface interaction [22]. This allows us to rank the stabilities of two-dimensional water structures to a high level of accuracy. An unbiased search for lowest-energy configurations based on seven different structural motifs has been performed. Sweeping across area densities, we can establish connections between different two-dimensional water structures, and gain insight into transitions to multilayer water. Additionally, water sheets with hexagonal, square and truncated-square motifs confined within graphene sheets have been studied in order to simulate realistic environments needed for the comparison with the experiment [10].

One- and two-layer-thick free-standing water structures were selected based on the simplest planar motifs – space-filling tilings of triangles, squares, rhombuses, rectangles, hexagons and octagons. The optimum area density of a given water layer was firstly estimated based on typical water-water distances and a probable structure that maximizes the ice rules [23]. Water molecules on these lattices were given random orientations, and then relaxed using conjugate gradient optimization. Up to 2048 initial configurations were used per motif in order to determine the arrangement of water molecules that minimizes energy. All water molecules were allowed to relax freely except for the triangular structure, in which the oxygen atoms had to be partially constrained in order to retain the triangular arrangement. All the water sheets shown in Fig. 1, with the exception of **rh(I)**, possess bilayer structure, i.e. not all atoms of one water layer are at the same height.

Starting with isolated clusters, the cyclic form of a water tetramer shown in Fig. 1a was found to be the most stable structure, in agreement with the current consensus in scientific literature [24–27]. Each water molecule is both a donor and an acceptor of a hydrogen bond in this structural isomer. In contrast, in the bilateral-symmetric $(H_2O)_4$ isomer (Fig. 1b) a water molecule is either donating, or accepting, two hydrogen bonds. There are two

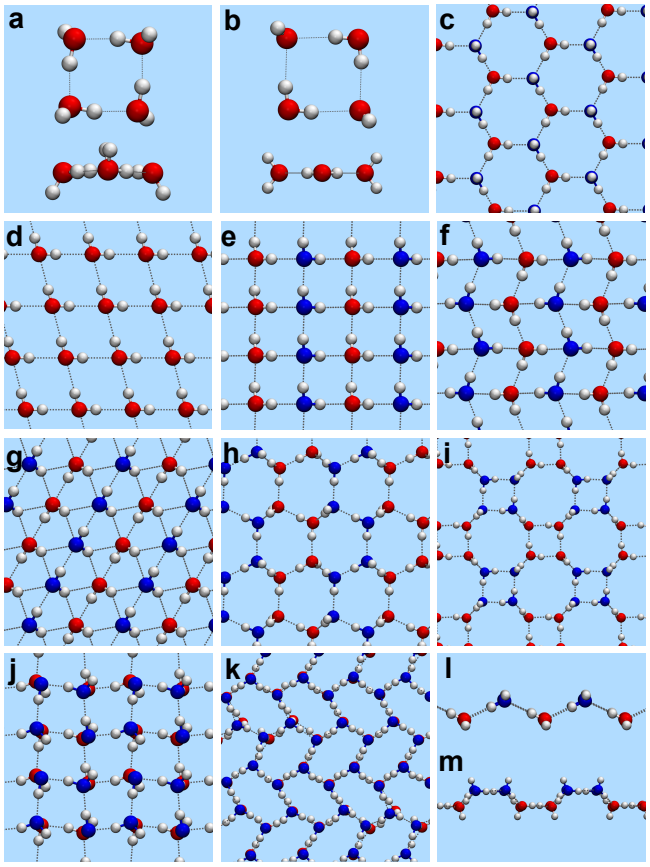

FIG. 1. Illustration of the motifs employed in the search for stable two-dimensional water structures. Water tetramers [**tet**]: (a) cyclic (up-down-up-down), (b) bilateral symmetric. Water sheets, where water molecules are ordered in an array of (c) regular hexagons, otherwise known as a hexagonal bilayer [**hex**], (d) rhombus, planar (with interior angles of 104.5°) [**rh(I)**], (e) squares [**sq**], (f) rhombic bilayer [**rh(II)**], (g) triangles [**tri**], (h) I_h secondary-prism bilayer [**sp**], (i) truncated-square bilayers [**tsq**], (j) two-layer square [**sq 2L**], (k) herringbone [**hb**], (l) squares (side view) and (m) truncated-square bilayers (side view). Blue/red coloring of oxygen atoms is used as an aid for visualizing corrugation (c-i) and distinguishing the two water layers (j,k). The sheets are shown at their optimum area densities, except for truncated-square bilayer (**tsq**) and the secondary-prism bilayer (**sp**) sheets, which are shown here at a density of ∼12.3 molecules/nm^2.

types of water molecules in this structure, based on their orientation: molecules which are flat-lying with respect to the tetramer plane, and molecules whose planes are normal to the tetramer plane.

Two-dimensional water structures based on hexagons, rhombuses, squares and triangles are illustrated in Figs. 1c-j. Figure 1h shows a bilayer water structure that projects onto a motif of irregular hexagons, resembling the $\{11\bar{2}0\}$/secondary-prism face of ice I_h. We hence name this two-dimensional water structure the secondary-prism water bilayer. In a competitive-growth method where the more stable face edges out the less stable, it was found that the secondary-prism face dominates at the ice-water interface [28]. Bilayer analogues of water sheets are lower in energy compared with their completely planar counterparts, regardless of the motif (see Supplementary information).

The truncated-square bilayer (Fig. 1i) is a hydrogen-bonded network of water tetramers. In contrast to the hexagonal bilayer, truncated-square bilayers do not have a net dipole moment along the direction normal to the water layer. Our calculations show that truncated-square bilayers consisting of bilateral-symmetric tetramers are energetically favored over truncated-square bilayers consisting of up-down-up-down or up-up-down-down cyclic tetramers.

The relative stabilities of one- and two-layer sheets of water measured in energy per molecule, plotted against area density are shown in Fig. 2 to illustrate how these ordered water structures may change as water is compressed laterally. In order to see this more clearly, we have defined area density as the total number of water molecules per unit area, regardless of how many layers of water comprise the sheet, or how corrugated a given water layer is. Motifs of most stable structures are illustrated at the bottom of the figure. Up to a density of 15.4 molecules/nm^2, one-layer (1L) structures are most stable whereas for higher densities two-layer (2L) structures become most stable.

Figure 2 demonstrates that the free-standing single hexagonal bilayer is not the structure of lowest total energy. At their respective optimum area densities, single-layer **sq** and **rh(II)** are more stable layers compared to the **hex** structure. Free-standing truncated-square bilayers and secondary-prism bilayers of water do not have an optimum area density, as compression readily leads to the formation of two-layer water sheets. These two water structures are, however, also lower in energy than the hexagonal bilayer. At the same time we point out that an infinite stacking of truncated-square bilayers is a metastable 3D water structure (Fig. 2) which can reconstruct into the more stable bulk I_h, consistent with what we expect from nature. The regular hexagon lattice has been the default structure assigned to water adsorbed on solid surfaces, most especially on hexagonal closed-packed metal surfaces [7]. Our results show that in fact a sufficiently strong coupling to a surface with hexagonal symmetry is required to form a single hexagonal water layer.

At area densities below 6.6 molecules/nm^2, water sheets comprised of interacting water tetramers were found to be most stable. This low-density region can be assigned to interacting clusters of water in general, which may not have a clear periodic structure. From 6.6 molecules/nm^2 onwards water forms an ordered lattice, beginning with a truncated-square structure, which possesses a fourfold-symmetric arrangement of oxygen atoms. This is replaced by the I_h secondary-prism structure, which has twofold symmetry, between 11.2 molecules/nm^2 and 15.4 molecules/nm^2.

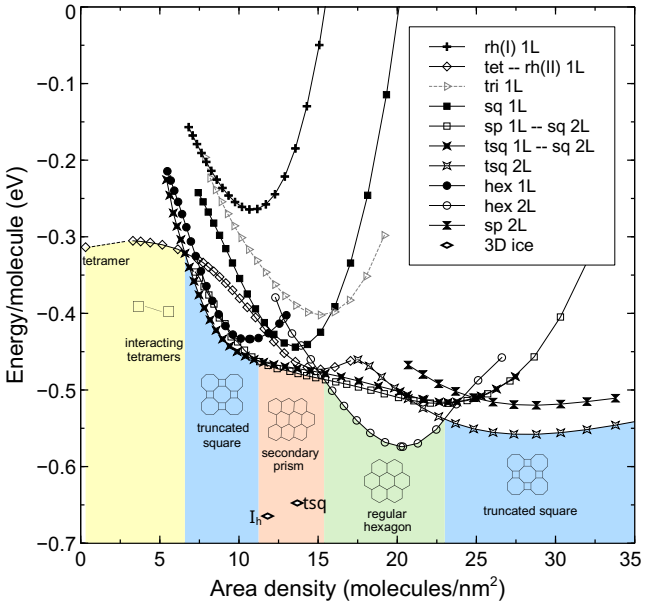

FIG. 2. Relative stabilities of one- (1L) and two-layer (2L) sheets of water. The plots are labeled according to the water structure exhibited at their respective energy minima. Motifs of the lowest-energy water structures at a given region of area density are shown. The formation energy of 3D ice **tsq** is plotted against the density of water molecules of a single form a truncated-square bilayer from this 3D crystal. Analogously, the area density used for I_h is that of the basal plane of the optimized solid.

A truly hexagonal water structure only becomes stable as a stacked two-layer system in the region of area density from 15.4 molecules/nm^2 up to 23.0 molecules/nm^2. This is in fact the most stable water sheet in energy per molecule among the one- and two-layer structures covered in this work, explaining its reported hydrophobicity [29], and the room-temperature order in interfacial water found using ab initio molecular dynamics [30]. Finally, at area densities greater than 23.0 molecules/nm^2, stacked truncated-square bilayers dominate among the water sheets that are only up to two layers thick.

What makes a particular water layer more stable cannot be attributed to a single factor – the number of O-H$\cdots$O linkages formed, their corresponding bond lengths, how linear these linkages are, the symmetry with respect to neighboring molecules, even the relative orientations of planes of individual water molecules all play roles, and these factors are *not* independent of each other. Stable 3D ice is formed when each water molecule donates two hydrogen bonds and accepts two hydrogen bonds, and when the four O-H$\cdots$O linkages are spatially separated in a tetrahedral geometry. Ice I_h – the most common form of ice we have on our planet – accomplishes this. As a case study in the two-dimensional domain, the **rh(I)** water layer is a completely planar sheet that one may naïvely designate as stable because of its network of linear O-H$\cdots$O linkages and perfect nearest-neighbor number of 4. However, the absence of some degree of intermolecular tetrahedral geometry makes this sheet an unfavored structure. This issue is resolved in the rhombic bilayer **rh(II)**, which is more stable than a hexagonal bilayer. The most stable single-layer water structures at densities between 11.2 molecules/nm^2 and 15.4 molecules/nm^2, the truncated-square bilayers and secondary-prism bilayers, are hydrogen-bonded to only 3 neighboring molecules, but they are arranged in a near-tetrahedral bonding geometry. For a two-layer structure of water, the coordination can be increased through interlayer bonding. This now renders the two-layer hexagonal structure to be most stable. Lastly, we mention that the water sheet **sq 2L** shown in Fig. 1j is only a metastable structure at 23.2 molecules/nm^2. Maximizing intra- and interlayer hydrogen bonding and tetrahedral coordination makes it impossible to form a perfect two-layer square lattice.

These results contribute to understanding water layers in contact with solid surfaces as they clarify the role of the water-water interaction in the structure formation. Note that on metal surfaces, a compensation effect between water-water and water-metal interaction has been found [5]: the stronger the water-metal interaction, the weaker the water-water interaction within the first layer and vice versa. This explains the stability of water layers at steps which are pinned at the metal step edge atoms but only weakly interacting with the metal atoms above the terraces so that a strong hydrogen-bonded network can form [8].

Recently, a square structure of water sandwiched between two graphene layer has been identified using high-resolution electron microscopy imaging [10]. There is still some ongoing discussion about the nature of the square structure that has been imaged [13, 14]. Still, it is instructive to look at possible water structures in such an arrangement from a theoretical point of view. Molecular dynamics simulations based on an empirical force field [10] proposed that square water arises from a bonding network best described by, but not identical to, the **rh(II)** layer in the current study, which we however find to considerably deviate from a square motif both at its optimum area density and at 12.3 molecules/nm^2 (Fig. 1f). The latter value corresponds to the density of water molecules per layer derived from the experiment [10].

In order to check whether confinement of water between graphene sheets influences the stability of the water structures, we have performed calculations for water layers adsorbed on graphene and trapped between two graphene layers. Note that the modeling of crystalline water layers between graphene sheets in a periodic setup requires finding an appropriate commensurate lattice for both subsystems. As the lattices of the considered water layers and graphene differ both in symmetry and size of their periodicities, we had to use unit cells containing up to 3096 atoms leading to a significant computational

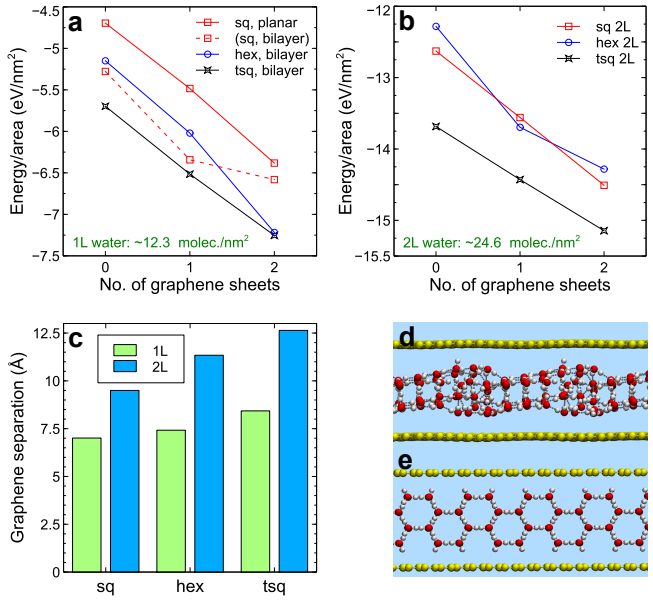

FIG. 3. Water adsorbed on, and confined within graphene sheets: (a) stability of one-layer water, (b) stability of two-layer water, (c) separation between graphene sheets confining water, (d) side view of confined **hex 2L** water, (e) side view of confined **tsq 2L** water. Initially square bilayer water on graphene and within two graphene sheets in panel (a) are in fact disordered water layers; the one-layer (1L) square sheet in (c) is accordingly of the planar form, which did not break down.

effort simulating these systems.

Figure 3a shows the relative stabilities of one-layer water with three different structures trapped between graphene sheets; Fig. 3b shows the analogue when another layer is added. At the experimentally derived water density per layer, we always find the truncated-square bilayers to be most stable, more stable than the hexagonal layers. Our water calculations do not predict any pure square structures of water to exist in nature.

Although the relative stability of the three motifs considered in Fig. 3 is unchanged upon confinement, we find that the additional stabilization through the graphene-water interaction depends on the particular geometry of the water layers. In order to understand formation energies better, it is useful to decompose the computed energies of the water layers into separate contributions from the water-graphene and the water-water interactions. The breakdown is listed in Table I. The interaction of a water layer with graphene is not negligible. It is weak [12] in comparison to bonding at water-metal interfaces. As one may expect, the role of graphene-water interaction in stabilizing confined ordered structures of water becomes less important with increasing water sheet thickness.

TABLE I. Breakdown of the energy of confined water sheets. All values are expressed in eV/nm^2. The ratio of the graphene-water contribution to the water-water contribution is also given.

system	graphene−water	water−water	ratio
hex, bilayer	-2.072	-5.146	0.403
sq, planar	-1.686	-4.696	0.359
tsq, bilayer	-1.451	-5.802	0.250
hex 2L	-2.000	-12.282	0.163
sq 2L	-1.880	-12.628	0.149
tsq 2L	-1.460	-13.685	0.107

Even if square water is not predicted to be most stable, it is interesting to test whether they are kinetically stabilized, i.e., whether their transformation is hindered by sufficiently large barriers. Square bilayer water readily broke down into a disordered structure on graphene and within two graphene sheets. Hexagonal sheets also reconstruct in order to minimize energy. At a density of 24.5 molecules/nm^2 the water sheet comprised of two hexagonal bilayers is markedly strained, by 73 meV/molecule. Graphene-water interaction destroys the double-bilayer network, forming a open non-planar structure (Fig. 3d). A more ordered two-dimensional structure that is similar in energy is the two-layer herringbone water sheet (Fig. 1k), which prefers a smaller confinement distance. The herringbone structure was found to be stable only within graphene confinement. On the other hand, we found that the two-layer sheet of square water confined in graphene is metastable – the order was not destroyed upon structure optimization even with 312 water molecules in the calculation.

The number of layers of water that comprise a confined ordered sheet of water is obviously connected to the size of the constricting framework. Molecular dynamics simulations using a 5-7 Å separation between graphene sheets produced ordered water sheets that are one-layer thick, while a 7-9 Å separation yielded two-layer water sheets [31, 32]. Our DFT calculations show that separation of graphene sheets is also strongly linked to the motif of the water sheet they enclose (Fig. 3c). Calculations predict that confined truncated-square bilayers are most stable at a graphene interlayer separation of 8.4 Å, while squares and hexagons prefer graphene separations less than 7.5 Å (Fig. 3c). One could argue that the separation of the two graphene sheets enclosing water is a factor that can be used to control the motif of water that is formed: square water is more favored when water is more constricted by the graphene sheets.

We have compared the stability of free-standing sheets of water for a wide range of area densities, and water sheets at similar surface area densities/surface coverages that are bounded by two graphene sheets. A search for the most stable two-dimensional ordered structures of water was done, covering seven structural motifs. Both the number of hydrogen bonds formed and intermolecular bonding at near-tetrahedral bonding angles were found important in determining structures with lowest energy.

Our calculations could not confirm the experimentally proposed pure square structure [10] of two-dimensional

water to be most stable. At the same time, we also did not find that hexagonal water layers are necessarily the most stable. Free-standing single water sheets with square, rhombus, truncated-square, and secondary-prism motifs were found to be lower in energy compared to the standard sheet in which water molecules are arranged in regular hexagons. Hence there might well be water structures in two dimensions that consist of motifs with a square geometry.

At the experimentally proposed density per water layer, we find one- and two-layer structures consisting of truncated-square motifs to be most stable, independent of the fact whether the water layers are free-standing, adsorbed on graphene or sandwiched between two graphene sheets. Thus we confirm the assertion of Ref. [10] that confined two-dimensional water can crystallize in a phase that has a symmmetry that is qualitatively different from the conventional hexagonal geometry of hydrogen bonding between water molecules. Our findings should aid future first-principles modeling of water at interfaces of arbitrary symmetries and interaction strengths, and we hope this work could encourage investigators to explore beyond hexagonal water at interfaces. Experimental verification of the existence of truncated-square, secondary prism and herringbone water structures is still being awaited.

METHODS

All DFT calculations were done using the RPBE functional [33] with the D3 scheme for computing dispersion effects using the form of the damping function proposed by Becke and Johnson [34]. This flavor of DFT was chosen because this has previously been shown to be good at describing the interaction between water molecules [21]. It is furthermore ideal for modeling interactions with graphene because of its good prediction of the graphene lattice constant, and also because of the inclusion of van der Waals interactions. The calculated lattice constant of 2.472 Å was used. This value is 0.5% larger than the graphite basal plane lattice constant 2.4589 Å derived from x-ray spectrometry [35]. For comparison, the lattice constant that PBE predicts is 2.467 Å, while RPBE-D3 using zero damping yields 2.480 Å. Calculations were performed using the code VASP using an energy cutoff of 450 eV, and a sufficient amount of k points. Water sheets are separated by at least 30 Å in the periodic supercell scheme. Structure relaxation calculations were terminated once the forces on all atoms became less than 0.01 eV/Å. Selected calculations repeated using the PBE functional and RPBE-D3 with zero damping yielded the same trends (see Supplementary information). PBE is known to overstructure water. Two water molecules in a periodic cell were used to model the water layer of regular hexagons. Four water molecules were used for the layers comprised of squares, rhombuses (i.e., rhombuses with acute interior angles) and triangles, while eight water molecules were used for truncated-square bilayers and secondary-prism bilayers.

Two types of periodic supercells were used in the calculations: rhombuses (for rhombus, regular hexagonal, and triangular motifs) and squares (square, rhombus, truncated-square, and secondary-prism motifs). Square water can be artificially predicted when the periodic unit cell is a square; but if water structures do not favor forming squares in a square unit cell, then this is surely not an artifact of the cell constraints.

By monitoring how the predicted minimum-energy structure evolves as a function of the number of random initial configurations, we estimate that for a system with four water molecules in the supercell, 200 initial configurations should be enough to obtain the global minimum structure to within an error bar of 1 meV. A system with eight water molecules requires about 1000 initial configurations to reach this level of accuracy.

Water sheet formation energies are expressed per molecule, and plotted with respect to the energy of a free water molecule, i.e. $E = 0$ when the water molecules are very far apart:

$$E_{\text{form}} = [E_{\text{sheet}} - NE_{\text{mol}}]/N \tag{1}$$

where E_{mol} is the energy of a free water molecule, E_{sheet} is the energy of the given water sheet, and N is the number of water molecules comprising the water sheet.

The graphene and water layers are structurally incommensurate, i.e. their different symmetries and lattice constants present a considerable mismatch. Working within this difficulty, the following water layer densities were used: 12.28 molecules/nm^2 for the square water sheet on graphene, 12.25 molecules/nm^2 for hexagonal water, and 12.40 molecules/nm^2 for truncated-square water. These values differ within 1.3% of each other. These surface densities were chosen in order to be as close as possible to the high packing density (12.49 molecules/nm^2) reported in Ref. [10] while minimizing system size, and hence computational cost. Square water was modeled using rectangles with an aspect ratio of 1.00074. Graphene sheets were stacked in an AB manner. Supercells containing up to 512 water molecules and 1560 carbon atoms were used in the calculations.

Water-graphene and water-water energy contributions were calculated using the following:

$$E(\text{graphene} - \text{water}) = [E_{\text{tot}} - 2E_{\text{g}} - E_{\text{H}_2\text{O-sheet}}]/A \tag{2}$$

$$E(\text{water} - \text{water}) = [E_{\text{H}_2\text{O-sheet}} - NE_{\text{H}_2\text{O-mol}}]/A \tag{3}$$

where E_{tot} is the energy of the full system in which water is confined within graphene, $E_{\text{H}_2\text{O-mol}}$ is the energy of a free water molecule, E_{g} is the energy of the graphene sheet, $E_{\text{H}_2\text{O-sheet}}$ is the energy of the given **hex**, **sq**, or **tsq** water layer, and A is the area of the supercell.

Finally, some conventions used in this paper: a *sheet* of water can be comprised of one to a few (in this work restricted to max. 2) *layers* – irreducible, ordered two-dimensional networks of water molecules. Layers that comprise a sheet are similar in structure, and are most stable when stacked directly upon each other. A single water layer can have a *bilayer* structure. Some papers use the term *bilayer* to denote a two layer-thick sheet of water. For clarity, we use the term *bilayer* to designate a layer that is a superposition of two distinct parallel planes containing water molecules. For a concrete example, Fig. 3e shows a sheet of water that is comprised of two truncated-square bilayers stacked upon each other, confined between graphene sheets.

ACKNOWLEDGMENTS

Useful discussions with Ossi Lehtinen, Tibor Lehnert and Ute Kaiser are gratefully acknowledged. Computational time at the bwForCluster for computational and theoretical chemistry JUSTUS of the bwHPC project of the Federal State of Baden-Württemberg and at the Leibniz-Rechenzentrum (LRZ) of the Bavarian Academy of Sciences are gratefully acknowledged.

AUTHOR CONTRIBUTIONS

AG directed and supervised the research project. TR designed the computational study and performed the electronic structure calculations. TR and AG wrote the paper.

[1] M. A. Henderson, Surf. Sci. Rep. **46**, 1 (2002).
[2] E. Spohr, Electrochim. Acta **49**, 23 (2003).
[3] D. Ortiz-Young, H.-C. Chiu, S. Kim, K. Voitchovsky, and E. Riedo, Nat. Commun. **4** (2013).
[4] J. Guo, X. Meng, J. Chen, J. Peng, J. Sheng, X.-Z. Li, L. Xu, J.-R. Shi, E. Wang, and Y. Jiang, Nat. Mater. **13**, 184 (2014).
[5] A. Groß, F. Gossenberger, X. Lin, M. Naderian, S. Sakong, and T. Roman, J. Electrochem. Soc. **161**, E3015 (2014).
[6] J. Chen, J. Guo, X. Meng, J. Peng, J. Sheng, L. Xu, Y. Jiang, X. Li, and E. Wang, Nat. Commun. **5**, 4056 (2014).
[7] A. Hodgson and S. Haq, Surf. Sci. Rep. **64**, 381 (2009).
[8] X. Lin and A. Groß, Surf. Sci. **606**, 886 (2012).
[9] M. J. Kolb, F. Calle-Vallejo, L. B. F. Juurlink, and M. T. M. Koper, JCP **140**, 134708 (2014).
[10] G. Algara-Siller, O. Lehtinen, F. Wang, R. Nair, U. Kaiser, H. Wu, I. Grigorieva, and A. Geim, Nature **519**, 443 (2015).
[11] R. R. Q. Freitas, R. Rivelino, F. de Brito Mota, and C. M. C. de Castilho, J. Phys. Chem. A **115**, 12348 (2011).
[12] J. L. Achtyl et al., Nat. Commun. **6**, 6539 (2015).
[13] W. Zhou *et al.*, Square ice in graphene questioned, Nature, http://dx.doi.org/10.1038/nature16145 (2015).
[14] G. Algara-Siller, O. Lehtinen and U. Kaiser, Algara-Siller *et al.* reply, Nature, http://dx.doi.org/10.1038/nature16149 (2015).
[15] A. K. Soper, Nature **519**, 417 (2015).
[16] A. Roudgar and A. Groß, Chem. Phys. Lett. **409**, 157 (2005).
[17] A. Michaelides, Appl. Phys. A **85**, 415 (2006).
[18] J. Carrasco, A. Hodgson, and A. Michaelides, Nat. Mater. **11**, 667 (2012).
[19] B. Hammer, L. B. Hansen, and J. K. Nørskov, Phys. Rev. B **59**, 7413 (1999).
[20] S. Grimme, J. Antony, S. Ehrlich, and H. Krieg, J. Chem. Phys. **132**, 154104 (2010).
[21] K. Forster-Tonigold and A. Groß, J. Chem. Phys. **141**, 064501 (2014).
[22] K. Tonigold and A. Groß, J. Comput. Chem. **33**, 695 (2012).
[23] J. D. Bernal and R. H. Fowler, J. Chem. Phys. **1**, 515 (1933).
[24] D. J. Wales and T. R. Walsh, J. Chem. Phys. **106**, 7193 (1997).
[25] M. P. Hodges, A. J. Stone, and S. S. Xantheas, J. Phys. Chem. A **101**, 9163 (1997).
[26] M. Masella, N. Gresh, and J.-P. Flament, J. Chem. Soc., Faraday Trans. **94**, 2745 (1998).
[27] J. F. Perez, C. Z. Hadad, and A. Restrepo, Int. J. Quant. Chem. **108**, 1653 (2008).
[28] M. J. Shultz, P. J. Bisson, and A. Brumberg, J. Phys. Chem. B **118**, 7972 (2014).
[29] G. A. Kimmel, J. Matthiesen, M. Baer, C. J. Mundy, N. G. Petrik, R. S. Smith, Z. Dohnlek, and B. D. Kay, J. Am. Chem. Soc. **131**, 12838 (2009).
[30] T. Roman and A. Groß, Catal. Today **202**, 183 (2013).
[31] W.-H. Zhao, L. Wang, J. Bai, L.-F. Yuan, J. Yang, and X. C. Zeng, Acc. Chem. Res. **47**, 2505 (2014).
[32] J. Bai and X. C. Zeng, Proc. Nat. Acad. Sci. **109**, 21240 (2012).
[33] B. Hammer, L. B. Hansen, and J. K. Nørskov, Phys. Rev. B **59**, 7413 (1999).
[34] S. Grimme, S. Ehrlich, and L. Goerigk, J. Comp. Chem. **32**, 1456 (2011).
[35] Y. Baskin and L. Meyer, Phys. Rev. **100**, 544 (1955).